

Dependence of Dielectric Layer and Electrolyte on the Driving Performance of Electrowetting-Based Liquid Lens

June Kyoo Lee^a, Kyung-Woo Park^{**a}, Hak-Rin Kim^{**a, b}, and Seong Ho Kong^{a, b}

Abstract

This paper presents the effects of a dielectric layer and an electrolyte on the driving performance of an electrowetting on dielectric (EWOD)-based liquid lens. The range of tunable focal length of the EWOD-based liquid lens was highly dependent on the conditions of the dielectric layer, which included an inorganic oxide layer and an organic hydrophobic layer. Moreover, experiments on the physical and optical durability of electrolyte by varying temperature conditions, were conducted and their results were discussed. Finally, the lens with a truncated-pyramid silicon cavity having a sidewall dielectrics and electrode was fabricated by anisotropic etching and other micro-electromechanical systems (MEMS) technologies in order to demonstrate its performance. The lens with 0.6 μm -thick SiO_2 layer and 10 wt% LiCl-electrolyte exhibited brilliant focal-length tunability from infinity to 3.19 mm.

Keywords: EWOD, liquid lens, dielectric, electrolyte, contact angle

1. Introduction

Electrowetting on dielectric (EWOD) is a noticeable actuation principle for micro-scaled devices without mechanical driving parts, such as micro-lens components, micro-pumps, micro-chip coolers, and flexible displays [1-4]. A droplet, below 2 mm in diameter, is affected dominantly by its interfacial tension (γ_{SL}) between liquid and solid rather than the gravitation, resembling a droplet hanging on the end of a leaf. The droplet on a dielectric layer can be changed to wetting or dewetting via control of the interfacial tension by electric fields across them as demonstrated in Fig. 1. Thus, the contact angle (θ) of a droplet can be continuously controlled by manipulating external voltage (V). The contact angle with external voltage is determined

by Lippmann-Young equation as shown below [5].

$$\theta(V) = \cos^{-1} \left[\cos \theta_0 + \frac{\epsilon_0 \cdot \epsilon}{2\gamma_{\text{LV}} \cdot t} V^2 \right], \quad (1)$$

where θ_0 is the contact angle at potential of zero charge, ϵ_0 is permittivity in vacuum, ϵ is dielectric constant, γ_{LV} is interfacial tension between liquid and vapor, and t is thickness of a dielectric layer. Based on this equation, the actuating performance is basically tunable by the physical properties of a dielectric material between the droplet and a metallic electrode. Many researchers have studied the relationship among a dielectric layer, an electrolyte, and electrowetting in pursuit of a lower driving voltage [6-8]. In this paper, silicon oxide, which is a widely applied dielectric material in metal-oxide-semiconductor field effect transistor (MOSFET)

Manuscript Received March 24, 2010; Revised June 11, 2010; Accepted for publication June 15, 2010

This research was financially supported by the Ministry of Education, Science Technology (MEST) and the Korea Institute for Advancement of Technology (KIAT) through the Human Resource Training Project for Regional Innovation. This was also partially supported by the National Research Foundation of Korea (2009-0088705).

* Member, KIDS; **Student Member, KIDS

Corresponding author: Seong Ho Kong

^a School of Electrical Engineering and Computer Science, Kyungpook National University, Daegu, Korea

^b School of Electronics Engineering, Kyungpook National University, Daegu, Korea

E-mail: shkong@knu.ac.kr Tel: +82-53-950-7579 Fax: +82-53-951-7579

Co-corresponding author: Hak-Rin Kim

E-mail: rineey@ee.knu.ac.kr Tel: +82-53-950-7211 Fax: +82-53-950-7211

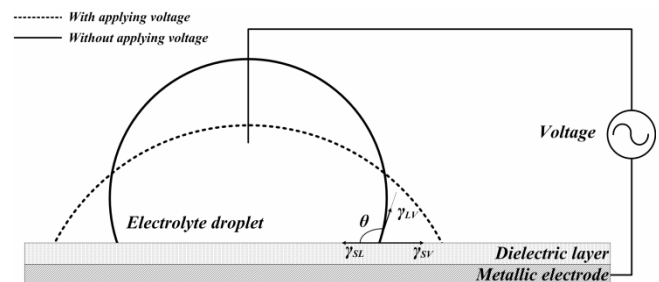


Fig. 1. Electrowetting of an electrolyte droplet on a dielectric layer.

and micro-electromechanical systems (MEMS) areas, was utilized as a dielectric layer for the EWOD.

As one of the useful applications, the focal-length tunable micro-lens driven by the EWOD has been researched by *B. Berge, B.H.W. Hendriks, et al.* [9, 10] since the early 2000s. The EWOD-based liquid lens has a wide range of industrial applications for miniature focus-tunable optical systems, i.e. mobile phone camera, capsule endoscope, and optical pickup head. These systems are driven by actuation of a free-standing conductive droplet in a micro-liter volume. The EWOD-based focal-length variable lens proposed in this paper is illustrated in Fig. 2. The lens is composed of two different types of droplet, lens body to contain the droplets, and two lens cover glasses for closing the droplets. As for the liquid droplet, two layers of immiscible liquids were used, where one is an electrolyte for electrowetting and the other is oil for protecting evaporation of the electrolyte. The oil is also for achieving graded refractive index lens effects by utilizing its high refractive index. With the confined structure, the gravitational effects on the liquid droplet shape can be minimized. In this paper, we describe the characteristics of contact-angle control depending on a dielectric layer including a hydrophobic layer with applied direct current (DC) voltage. We also present the physical and optical characteristics of electrolytes for efficient and reliable actuation in the EWOD-based liquid lens. Finally, we demonstrate the performance of a realized MEMS-based liquid lens driven by EWOD using experimental results.

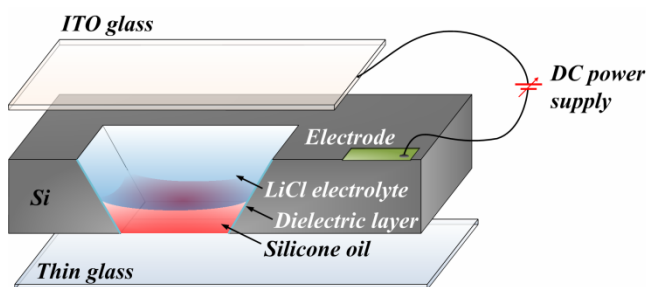


Fig. 2. Schematic of the EWOD-based focal-length variable liquid lens composed of two different types of droplet, lens body to contain the droplets, and two lens cover glasses for closing the droplets.

2. Experiments

To compare the dependence of the dielectric layer's dielectric constant on the EWOD actuation, silicon oxide and

aluminum oxide layers of 2 μm are deposited on an indium tin oxide (ITO, $3.2 \Omega/\square$)-coated glasses by plasma enhanced chemical vapor deposition (PECVD, Oxford Plasmalab system 100) and by atomic layer deposition (ALD, NCD Lucida D100), respectively. To determine an optimized dielectric condition, the thickness of silicon oxide layer was changed from 60 nm to 1800 nm in this study. A hydrophobic layer was then coated onto the oxide layers. The hydrophobic layer plays a role in making a large initial contact angle and lubrication in a droplet's movement. In this paper, tetrafluoroethylene (DuPont Teflon[®] AF 1601) was spin-coated at 6000 rpm for 30 seconds and polymerized at 330 $^{\circ}\text{C}$ for 15 minutes. Its thickness was modulated by a change in solids concentration in the solvent (3M FC-40). Moreover, the effect of hydrophobic layer thickness on electrowetting performance was simulated. Fig. 3 shows the experiment setup used in this work. An external voltage was applied between the metal tip immersed into the droplet and the ITO electrode using direct current (DC) power supply (KEITHLEY 2400 Source Meter). The droplet's contact angle was measured using a drop shape analyzer (KRÜSS DSA 100).

In this study, we also checked the dependence of electrolyte on the physical and optical characteristics of the EWOD-based liquid lens. The electrolyte droplet was an aqueous solution composed of lithium chloride (LiCl), de-ionized water, and surfactant. LiCl has good solubility in water and excellent endurance against liquid freezing. A surfactant was added to reduce interfacial tension (γ_{LV}) of the solution for enhancing the electrowetting performance as stated above in Eq. (1). Among the components of the solution, salt concentration was regulated to 1, 10, and 20 wt%, respectively. Table 1 demonstrates the conditions of

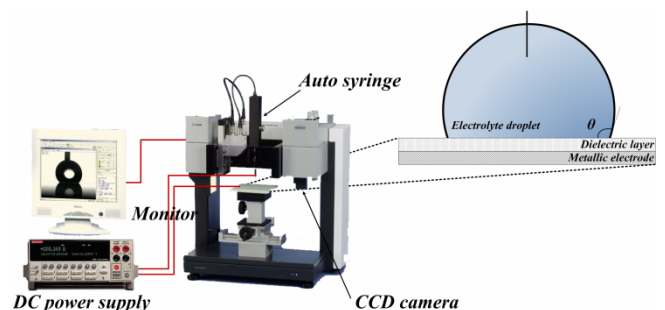


Fig. 3. Experiment setup for analyzing contact-angle change in the droplet by electrowetting.

Table 1. Concentration ratios of electrolytes.

Types of electrolyte	Concentration ratio (wt%)		
	H ₂ O	LiCl	1,2-propanediol
Electrolyte 1	69	1	30
Electrolyte 2	60	10	30
Electrolyte 3	50	20	30

the mixed solution in detail. The first group of the mixed solutions was placed in a refrigerator and kept at -24 °C and -62 °C for 40 hours, respectively. Phase transition of the solutions was then observed. The second group of the solutions was regulated with various temperatures at -24 °C, -62 °C, and 90 °C for 40 hours, respectively. Temperature was subsequently returned to room temperature. Finally, its optical transmittance in the visible range of 380-750 nm was measured and compared with the reference solution. When an optimized concentration ratio of the electrolyte was chosen, we fabricated a focal-length tunable liquid lens driven by electrowetting using silicon MEMS technology. The thickness of silicon oxide layer was applied with 20, 600, and 1500 nm, respectively, using the same hydrophobic layer condition. The electrolyte was composed of 60 wt% deionized water, 30 wt% 1,2-propanediol, and 10 wt% LiCl. Then, lens performance was analyzed by applying DC voltage.

3. Results and Discussion

3.1 Dependence of dielectric layer on electrowetting performance

Fig. 4 shows the contact angle characteristics on a silicon oxide layer and an aluminum oxide layer as a function of applied voltage. Because the dielectric constant of aluminum oxide is almost two-and-a-half times higher than that of silicon oxide, the contact angle's tunability is better for aluminum oxide dielectrics at the same applied voltage. However, durability of the deposited aluminum oxide layer was not promising enough to avoid breakdown over 40 V compared to that of the silicon oxide layer [11]. Fig. 5 shows the contact angle behavior at 40 V depending on the silicon oxide layer thickness. As expressed in Eq. (1), the contact angle change is decreased parabolically as silicon oxide layer thickness increased. However, in 60-80 nm thin

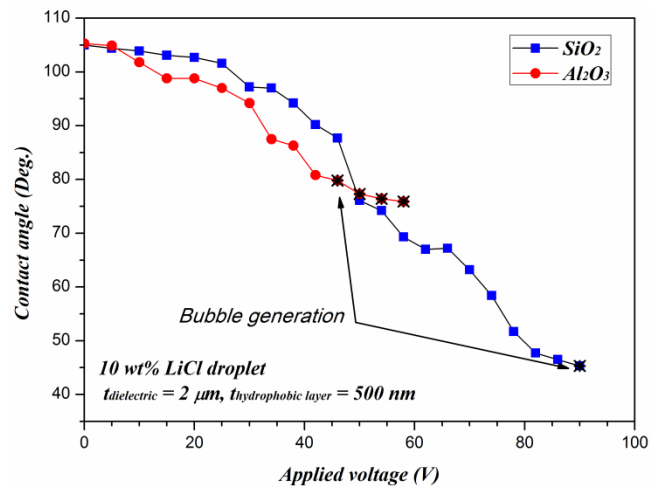


Fig. 4. Contact-angle characteristics of SiO₂ layer and Al₂O₃ layer as a function of applied voltage.

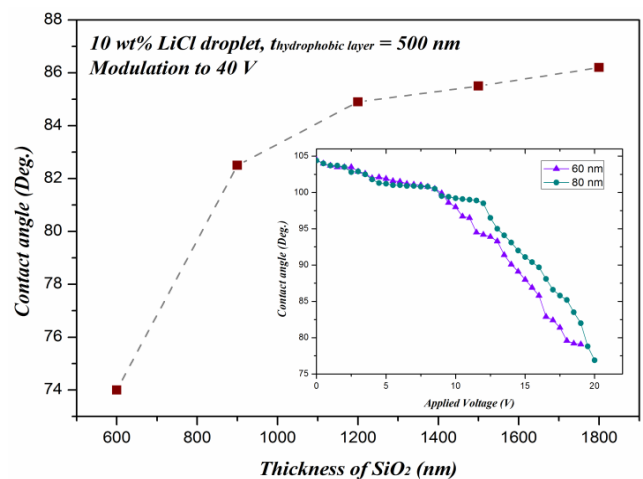


Fig. 5. Contact angle change at 40 V as a function of the silicon oxide layer thickness.

film, breakdown easily occurred at the high contact angle region before 40 V. Thus, 600-nm-thick silicon oxide layer at the very least is adequate for liquid lens application with a contact angle change of 40°. Fig. 6 presents the simulated capacitance in unit area as functions of a hydrophobic layer thickness and thickness control of the hydrophobic layer by its concentration of solids in solvent. As shown in the calculated data, a thicker hydrophobic layer produces a less coupling capacitance, resulting in a less influencing power of dielectric constant in the EWOD system. Because the tetrafluoroethylene layer has a low dielectric constant of about 1.93, the total capacitance of the system had to be reduced.

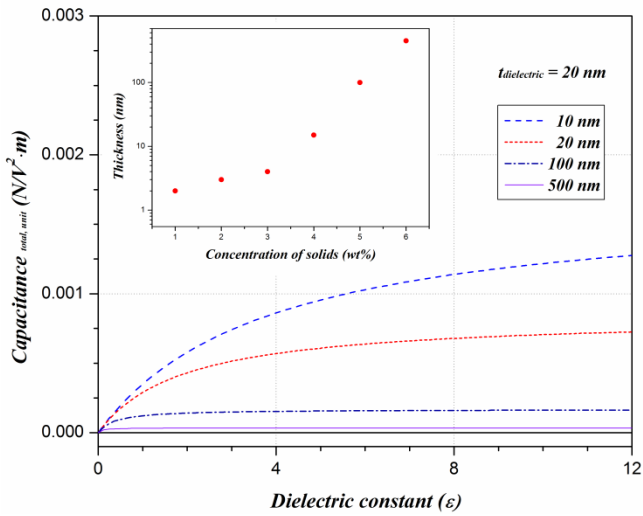


Fig. 6. Simulated capacitance in unit area as functions of the hydrophobic layer thickness and its thickness control by concentration modulation of solids in solution.

Thus, the thickness of the hydrophobic layer should be minimized in order to optimize the effect of dielectric constant on the EWOD system. In this work, tetrafluoroethylene layer of 4 wt% solids was suitable due to its hydrophobicity and thinness. In the layers less than 3 wt% of solids, their thicknesses were decreased gradually but their hydrophobicity was poor due to low surface uniformity and generated micro-pores. In contrast, the layers were as thick as the total capacitance of the system was reduced when more than 5 wt% of solids was used.

3.2 Dependence of electrolyte on lens performance

Table 2 denotes phase transitions of the mixed solutions at low temperature for 24 hours. All solutions were kept at liquid phases until -24 °C. When the solutions were cooled down to -62 °C, only electrolyte 3 remained in the liquid phase, while electrolyte 1 and electrolyte 2 were fro-

Table 2. Phase transitions of electrolytes in extremely low temperature.

Types of electrolyte	Temperature	
	-24 °C	-62 °C
Electrolyte 1	Liquid	Solid
Electrolyte 2	Liquid	Solid
Electrolyte 3	Liquid	Liquid

zen. The result demonstrates that an increase in electrolyte salt concentration promises durability in the phase transition, which is a critical problem in liquid-based micro-lens performance. However, electrolyte solution with heavy salt concentration lowers the electro-wetting characteristics by virtue of the thick, electrical double layer (EDL) as well as by the active penetration of ions from an electrolyte into an oil droplet at the interface [12]. Fig. 7 shows the optical transmittance of the electrolytes at room temperature. Even though electrolyte 2 revealed slightly low transmittance in the range of 380-650 nm, all the electrolytes had good optical transmittance over 92%/cm in the whole wave-length range. Fig. 8 demonstrates the optical results of the electrolytes after the experiment on extreme temperature change. All electrolytes had good properties in transmittance over 95 %/cm in any temperature change and any salt concentration in this work. Transmittances in all samples tended to be lowered gradually as the wavelength became longer. These results reflect that constraint of phase transition and reinforced transmittance at the red color range are the most considerable points for enhancing lens performance. Although the increase in LiCl enhances resistance against phase transition in low temperature, excessive ions in an electrolyte induces mixture with an oil in the interface region, which degrades the performance of an electro-wetting-based lens. We finally selected the electrolyte of 10 wt% LiCl (electrolyte 2) and applied it for the lens in this work.

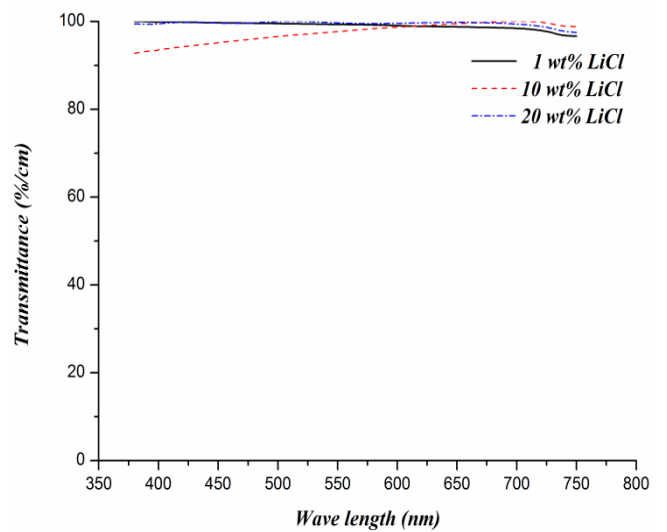


Fig. 7. Transmittance in the range of 380-750 nm of the electrolytes at room temperature.

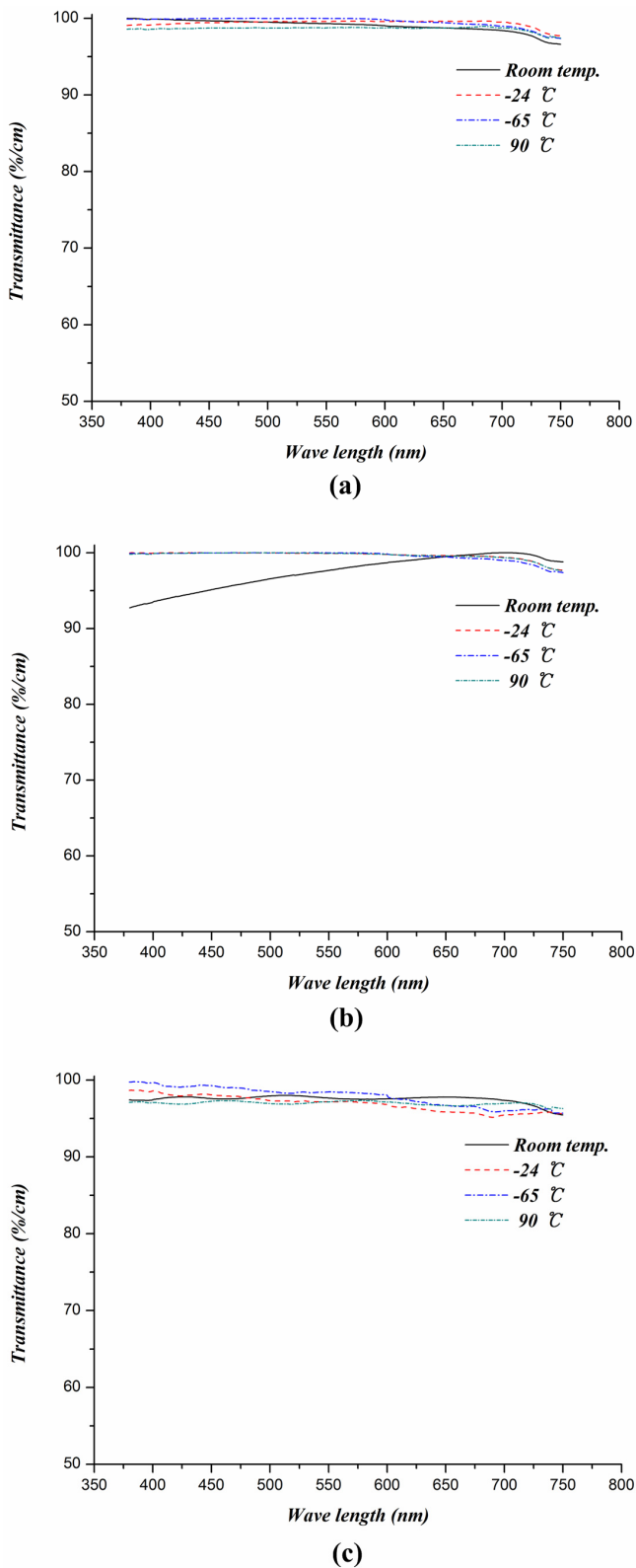


Fig. 8. Transmittance results of the electrolytes after extreme temperature change. (a) - (c) are the electrolytes of 1, 10, and 20 wt% LiCl respectively.

3.3 Lens fabrication and performance

We fabricated three MEMS-based liquid lenses, actuated by EWOD, and designed the dielectric layer and electrolyte of the lens based on the results stated above. First, the silicon lens cavities to contain liquid droplets were fabricated in the form of a truncated pyramid by anisotropic silicon wet etching using trimethylammonium hydroxide (TMAH) solution. The cavity sizes of the top side were $1.5 \times 1.5 \text{ mm}^2$ while their heights were about $700 \mu\text{m}$. The 500-nm -thick silicon oxide layers were grown on the sidewall of the cavities through wet oxidation as an electrical passivation layer. The sidewall electrodes were then formed with aluminum by e-beam evaporation. On the metal electrodes, the $20, 600, \text{ and } 1500 \text{-nm}$ -thick silicon oxide layers, as a dielectric layer for the EWOD, were deposited by PECVD, respectively. The cavities were spin-coated with tetrafluoroethylene. The bilayer of liquids with silicone oil of $0.5 \mu\text{l}$ and a LiCl electrolyte of $1.5 \mu\text{l}$ were used. Fig. 9 illustrates the summarized fabrication process and the fabricated lens. Fig. 10 shows the actuating performance of the lens, which was controlled by a curvature change in the electrolyte droplet using electrowetting. A printed object on transparent poly(chloroethanediyl) film was located under the lens and its pattern was observed through the fabricated lens. The oil droplet changed its shape from concave to convex due to wetting of the electrolyte droplet in the lens cavity. Because the refractive index of an oil droplet is larger than that of an electrolyte droplet, the object was zoomed in when the oil droplet was changed into convex shape. The pattern was magnified about 1.5 times as shown in Fig. 10. Driving performance for acquisition of a 1.5

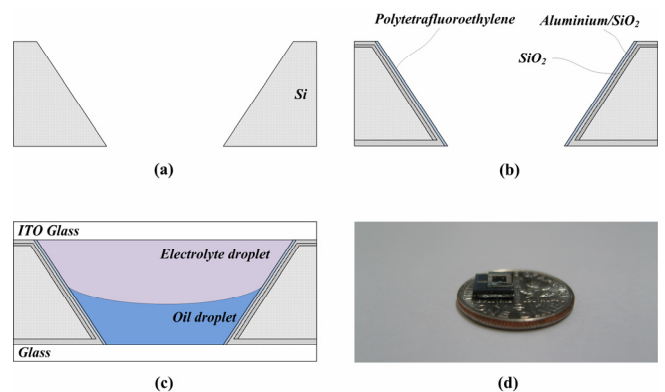


Fig. 9. Schematics of fabrication process and photograph of the fabricated lens.

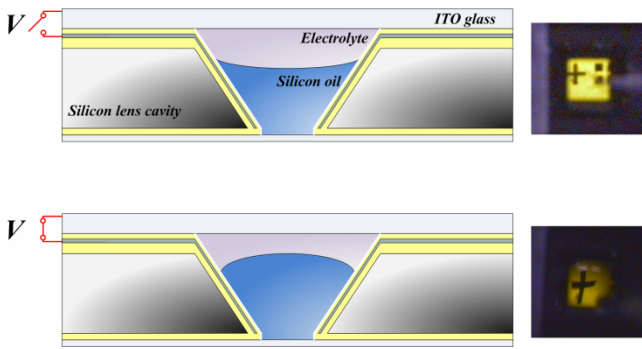


Fig. 10. Actuation of the fabricated lens with applying voltage of 50 V.

times magnified image is denoted in Table 3. The driving voltage of the fabricated lens rose higher than that of a flat substrate with air ambient due to friction between the oil droplet and sidewall. Moreover, the driving voltage was reduced with thinning of the dielectric layer. However, the lens with the 20 -nm-thick silicon oxide layer malfunctioned. Fig. 11 demonstrates the optical performance of the fabricated lens with a 600 -nm-thick silicon oxide layer and 10 wt% LiCl-electrolyte. When the voltage reached 10 V, the image size was the same as the object size. With a further rise in voltage, the object is magnified to 1.78 times its actual size. Compared with other micro-lenses based on electrostatic force, the lens exhibited brilliant optical performance with high focal-length tunability from infinity to 3.19 mm [13-15]. Electric power consumption was determined to be less than 1mW.

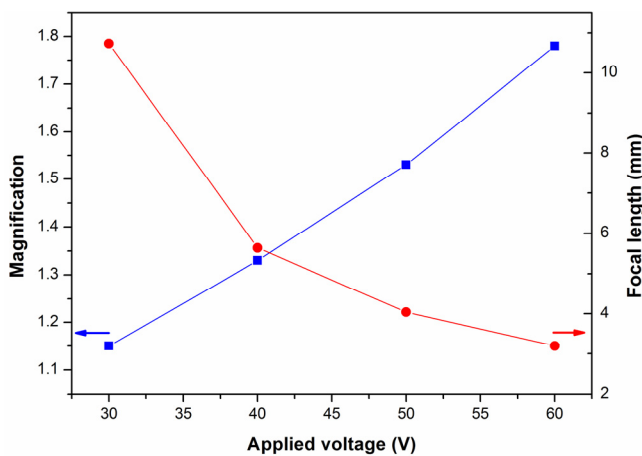


Fig. 11. Magnification and focal length characteristics of the fabricated lens as a function of applied voltage.

Table 3. Driving voltage of the fabricated lens for 1.5 times magnification

Lens model	Thickness of dielectric (nm)	Driving voltage (V)
Lens 1	1500	77
Lens 2	600	50
Lens 3	20	Malfunction

4. Conclusions

In this paper, dielectric layer and electrolyte dependence on the driving performance of an electrowetting-based liquid lens was discussed. A EWOD-based tunable lens was fabricated using MEMS technology. Prior to fabrication of the lens, we conducted not only some experiments with flat ITO-coated substrates in order to find out brilliant conditions related to dielectric and hydrophobic layers, but also tested the physical and optical durability of electrolyte in extreme temperature conditions. We employed silicon oxide as a dielectric layer for EWOD due to the relatively higher breakdown strength compared to the aluminum oxide layer, in spite of its lower permittivity. Because EWOD is conducted on a stacked insulator composed of two layers, silicon oxide and hydrophobic layers, the hydrophobic layer has to be minimized to enhance the lens' driving performance. In this work, we could get an approximately 10 -nm-thick tetrafluoroethylene layer using spin-coating conditions with a solution of 4 wt% solids and 6000 rpm for the most suitable electrowetting performance. An electrolyte of 10 wt% LiCl was appropriated for liquid-based micro-lens due to its good optical transmittance at various temperature shocks in the range of visible ray. It is demonstrated that the fabricated lens could magnify an object 1.78 times with 60 V of DC bias.

References

- [1] B. Hendriks and S. Kuiper, *IEEE Spectr.* **41**, 32 (2004).
- [2] K. -S. Yun, I. -J. Cho, J. -U. Bu, C. -J. Kim, and E. Yoon, *J. Microelectromech. Syst.* **11**, 454 (2002).
- [3] P. Y. Paik, V. K. Pamula, and K. Chakrabarty, *IEEE Des. Test Comput.* **25**, 372 (2008).
- [4] R. A. Hayes and B. J. Feenstra, *Nature* **425**, 383 (2003)
- [5] F. Mugele and J. -C. Baret, *J. Phys. -Condes. Matter* **17**, R705 (2005).
- [6] H. Moon, S. K. Cho, R. L. Garrell, and C. -J. Kim, *J. Appl. Phys.* **92**, 4080 (2002).

- [7] S. Berry, J. Kedzierski, and B. Abedian, *J. Colloid Interface Sci.* **303**, 517 (2006).
- [8] A. Quinn, R. Sedev, and J. Ralston, *J. Phys. Chem. B* **107**, 1163 (2003).
- [9] B. Berge and J. Peseux, *Eur. Phys. J. E* **3**, 159 (2000).
- [10] S. Kuiper and B. H. W. Hendriks, *Appl. Phys. Lett.* **85**, 1128 (2004).
- [11] J. Kolodzey, E. A. Chowdhury, T. N. Adam, G. Qui, I. Rau, J. O. Olowolafe, and J. S. Suehle, *IEEE Trans. Electron Devices* **47**, 121 (2000).
- [12] Y. S. Nanayakkara, H. Moon, T. Payagala, A. B. Wijeratne, J. A. Crank, P. S. Sharma, and D. W. Armstrong, *Anal. Chem.* **80**, 7690 (2008).
- [13] S. Xu, Y. J. Lin, and S. T. Wu, *Opt. Express* **17**, 10499 (2009).
- [14] C. C. Cheng, and J. A. Yeh, *Opt. Express*. **15**, 7140 (2007).
- [15] B. Berge, *Nikkei Electronics* **911**, 129 (2005).